Stochastic Multiconfigurational Self-Consistent Field Theory

Robert E. Thomas,*,† Qiming Sun,‡ Ali Alavi,†,¶ and George H. Booth*,§

†The University Chemical Laboratory, University of Cambridge, Lensfield Road, Cambridge CB2 1EW, United Kingdom
‡Department of Chemistry, Princeton University, Princeton, New Jersey 08544, United States
¶Max Planck Institute for Solid State Research, Heisenbergstraße 1, 70569 Stuttgart, Germany
§Department of Physics, King's College London, Strand, London WC2R 2LS, United Kingdom

ABSTRACT: The multiconfigurational self-consistent field theory is considered the standard starting point for almost all multireference approaches required for strongly correlated molecular problems. The limitation of the approach is generally given by the number of strongly correlated orbitals in the molecule, since its cost will grow exponentially with this number. We present a new multiconfigurational self-consistent field approach, wherein linear determinant coefficients of a multiconfigurational wave function are optimized via the stochastic full configuration interaction quantum Monte Carlo technique at greatly reduced computational cost, with nonlinear orbital rotation parameters updated variationally based on this sampled wave function. This extends this approach to strongly correlated systems with far larger active spaces than it is possible to treat via conventional means. By comparison with this traditional approach, we demonstrate that the introduction of stochastic noise in both the determinant amplitudes and the gradient and Hessian of the orbital rotations does not preclude robust and reliable convergence of the orbital optimization. It can even improve the ability to avoid convergence to local minima in the orbital space, and therefore aid in finding variationally lower-energy solutions. We consider the effect on the convergence of the orbitals as the number of walkers and the sampling time within the active space increases, as well as the effect on the final energy and error. The scope of the new protocol is demonstrated with a study of the increasingly strongly correlated electronic structure in a series of polycyclic aromatic hydrocarbons, up to the large coronene molecule in a complete active space of 24 π electrons in 24 orbitals, requiring only modest computational resources.
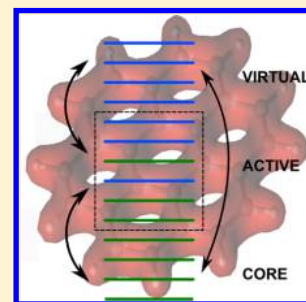
INTRODUCTION

Much of the fields of computational electronic-structure theory and quantum chemistry are concerned with describing the changes in energies and properties that are due to the correlated motion of electrons.[1] The treatment of these effects is generally required for the fields to be predictive and increasingly relevant to wider areas of chemistry, physics, and material science. This correlated physics of the electrons is generally divided into two qualitative categories: *dynamic* and *static* correlation.

As a broad categorization, dynamic correlation describes the short-ranged, two-electron phenomena of the Coulomb holes and cusps denoting the depletion in probability amplitude of finding two electrons close to each other. Static correlation, on the other hand, derives from the breakdown in the qualitative utility of the single-particle picture, which manifests as strong mixing between several determinants, with many-body co-operative effects giving rise to significant probability amplitudes of the wave function among its energetically low-lying configurations. If an electronic system contains significant static correlation, then perturbative approaches such as the "gold standard" of quantum chemistry—coupled-cluster with singles, doubles, and noniterative triples (CCSD(T))—will necessarily fail, since they rely on the single-particle picture to generate a single many-electron state about which to construct a perturbative expansion. This situation is prevalent in systems with localized, partially occupied atomic states (such as the *d*-

shells of transition metals), as well as low-spin, open-shell systems (including magnetic interactions) and important transition or stretched-bond configurations of molecular systems.

In quantum chemistry, it can be common to *define* the amount of static correlation in a problem as the difference between the uncorrelated Hartree–Fock energy and that of complete active space self-consistent field (CASSCF) theory. The CASSCF method is a variational approach for optimizing a linear combination of low-energy configurations which arise from a set of correlated "active" degrees of freedom, optimized self-consistently to provide the majority of the static portion of the correlation effects.[2−10] This is then considered as the standard starting point for almost all multireference approaches required for strongly correlated molecular problems. Many "active" orbitals and electrons are chosen, and the configurational subspace is constructed from all the possible distributions of those electrons in those orbitals, maintaining an inert "core" of the remaining particles. The energy is then minimized within this configurational subspace. In addition to this, a unitary rotation of the nonredundant orbital space is found, again in a variational fashion, in order to optimize the "best" orbitals, in a variational sense, to describe these configurations. This optimization can be crucial, since the original orbitals are

generally based on the canonical Hartree–Fock orbitals and, hence, do not necessarily span the qualitatively correct degrees of freedom to describe the strongly correlated physics.

Since the high-energy part of the configurational spectrum is missing, this approach will not, with normal usage, be able to capture dynamic correlation from high-energy virtual scattering effects to obtain a complete description of the correlated wave function. However, the final CASSCF wave function will achieve a qualitative description of a strongly correlated molecular problem, which will have been previously missing if building upon a single-reference. Dynamic correlation can often be included subsequently in the description on top of a CASSCF "zeroth-order" wave function in a perturbative or variational manner.[11−13]

The greatest limitation upon the applicability of the CASSCF approach is the size of the active space that can be treated. While this space would, ideally, include all valence electrons and low-lying molecular orbitals, the resultant number of variational parameters to optimize grows factorially with its size. Thus, computational bottlenecks usually demand that no more than ∼16 active electrons and degrees of freedom can be considered to contribute to the strong correlation. For larger systems with multiple stronger correlation centers, this is often simply insufficient, and even for relatively small systems, testing the influence of additional effects such as "s−p" mixing or a double-d-shell to include d−d transitions and wider energy scales in metal complexes is generally prohibitively expensive.

In order to access these required larger space sizes, approximations are generally made to reduce the number of parameters that must be optimized. The most prevalent of these are the *restricted* active space,[14,15] and, more recently, the *generalized* active space constructions.[16−19] These approaches choose only a subset of the complete active space configurations within which to optimize, thereby dramatically cutting the number of configurations that must be considered. However, this adds additional uncertainties and approximations in the quality of the results, as well as additional complexity in setting up the calculation.

To maintain the full variational flexibility of the active space and the treatment of strong correlation effects which that entails, we adopt a different approach in this work. The optimization of the linear determinant coefficients is decoupled from the nonlinear orbital rotation parameters. The linear coefficients are then solved stochastically for each iteration, using the machinery of the full configuration interaction quantum Monte Carlo (FCIQMC) method.[20] Stochastically derived quantities have been previously used for quantum chemical methods,[21−23] and FCIQMC provides a probablistic approach to the solution of the configuration interaction (CI) problem, whereby sparsity in the wave function is exploited to allow for large numbers of determinants to be optimized in systems for which a deterministic solution (or even enumeration of the space) would be impossible. Simultaneous to this sampling, one- and two-body reduced density matrices are accumulated, which are used in a subsequent step to form the gradient and Hessian for the orbital rotations among the active and inactive spaces. The rotations are then solved for deterministically (using the stochastically sampled gradient and Hessian), since there are generally a manageable number of these variational parameters, which grow only as $O[M^2]$, where M is the total number of orbitals in the full space. This process is repeated until convergence, implicitly coupling the linear parameters of the active space back to the nonlinear rotations within the full space.

We begin with a more-detailed discussion of these steps, before comparing the new approach to traditional techniques. Of particular interest is how the systematic and random errors of the result are dependent on the number of walkers, and on the amount of time for which these walkers stochastically sample the active space in the FCIQMC step, as well as an analysis of the nature of the convergence over updates of the nonlinear parameters. Moving beyond what can be feasibly optimized within traditional CASSCF, we turn to a series of increasingly large polycyclic aromatic hydrocarbons. These are important systems in the development of new photovoltaic devices,[24,25] while the trend from molecular systems toward the infinite graphene system and its novel properties is also of interest.[26,27] However, as the conjugated π system grows in size, there is no natural separation of energy scales from which an active space can be formed, and so the problem of a balanced choice of active space with which to compare systems of different sizes traditionally becomes difficult. With this new approach, however, we can consider the complete π space in all cases, allowing for a consistent truncation of the correlation effects, and we can examine trends as these systems grow in size. Density matrix renormalization group (DMRG) calculations have previously indicated a trend for increasing strong correlation effects, toward polyradical character, in one-dimensional polycyclic acenes and narrow nanoribbons,[28,29] and we compare this to the character of growth in two-dimensional (2D) polycyclic systems, up to the $C_{24}H_{12}$ coronene system, including all 24 π electrons and orbitals in the active space. It is found that, while there is a general increase in correlated behavior with increasing system size, the 2D series also sees the development of degeneracies in the highest-occupied and lowest-unoccupied parts of the natural orbital spectrum not observed in the linear cases.

■ METHODOLOGY

The wave function of MCSCF theory is ultimately expressed as a linear combination of N-electron Slater determinants, $\{|D_i\rangle\}$. However, its crucial difference from a wave function expanded as a subset of configurations involves the inclusion of an orbital rotation operator, $e^{-\hat{\kappa}}$, to allow for the iterative optimization of the space spanned by the correlated orbitals, in addition to the set of configurational coefficients, $\{C_i\}$, within it:

$$|\Psi\rangle = e^{-\hat{\kappa}} \sum_i C_i |D_i\rangle \tag{1}$$

The anti-Hermitian operator ($\hat{\kappa}$) takes the form of a sum over antisymmetrized excitation operators, which, in this work, we take to be spin-free:

$$\hat{\kappa} = \sum_{pq} \kappa_{pq} \hat{E}_{pq}^- \tag{2}$$

$$= \sum_{pq} \kappa_{pq} (\hat{E}_{pq} - \hat{E}_{qp}) \tag{3}$$

with

$$\hat{E}_{pq} = \hat{a}_{p\alpha}^\dagger \hat{a}_{q\alpha} + \hat{a}_{p\beta}^\dagger \hat{a}_{q\beta} \tag{4}$$

such that the rotations are real and preserve spin. Thus, the task is to determine the coefficients, $\{C_i\}$, and the matrix elements, $\{\kappa_{pq}\}$.

It is specifically the complete-active-space (CASSCF) treatment, which truncates the configurational space by partitioning the orbital space into inactive, active, and virtual subspaces, with which we are concerned here. No restrictions are placed on the allowed occupancies in the active manifold, but the inactive and virtual orbitals are constrained to be always doubly occupied and unoccupied, respectively, in all configurations. The related restricted-active-space (RASSCF) theory, which further divides the active space by placing restrictions on the number of holes and electrons allowed to appear at its lower and upper energetic limits, is also implemented, and this theory will be considered in future work. In CASSCF, simplifications arise as all intraspace rotations (active−active rotations, for instance) are redundant, while all interspace transformations are not.[1] Therefore, the only transformations that need to be considered are inactive−virtual, inactive−active, and active−virtual rotations, which induces a sizable reduction in the effective size of the matrix κ.

In principle, CASSCF may be undertaken as a simultaneous second-order optimization of the orbital and configurational parameters. While some of the established CASSCF implementations take this approach,[7,8,30−32] it restricts the flexibility for using newly developed solvers for strongly correlated quantum problems to obtain the CI coefficients. Increasingly, therefore, a two-step, macroiterative approach, in which the configurational and orbital parameters are optimized separately, has come into prominence. These approaches are predicated on the fact that the equations governing configurational optimization are equivalent to those found in "standalone" CI theory, and may thus be solved with any of the techniques which seek to approximate it. The approach using DMRG as the configurational solver has enjoyed considerable success,[33−37] with studies on long-chain polyenes, β-carotene, and transition-metal clusters all proving fruitful, and the stochastic approach discussed here ultimately seeks to continue in that vein.

Our formulation uses the full configuration interaction quantum Monte Carlo (FCIQMC) technique as its configurational optimizer, which we have elucidated in previous work.[20,38−45] This approach achieves the stochastic integration of the underlying Schrödinger equation via an imaginary-time evolution of an ensemble of signed walkers in Slater-determinant space. This evolution is performed as an iterative application of "spawning", "death", and "annihilation" steps, with the effect that the walker populations on each determinant, $\{N_i\}$, become proportional to the coefficient, $\{C_i\}$, when averaged over the long-imaginary-time limit. To control the sign problem, the initiator approximation is used, which results in a method that exhibits a systematic error at walker numbers that are too low, but which is systematically improvable to exactness as the number of walkers increases. Throughout this work, the initiator threshold parameter, n_a, is chosen to be 3.[38] To further reduce the size of random error bars, we make use of the semistochastic adaptation, in which the projection operator for the ground-state is applied deterministically to a small, "core" space, and stochastically elsewhere.[46,47] For the systems studied here, we choose our core spaces to be either all the determinants coupled to the reference, or 1000 such objects, whichever is smaller.

Crucially for our present purposes, the FCIQMC approach also facilitates the stochastically unbiased sampling of the two-body reduced density matrices (RDMs),[48,49] given by

$$\Gamma_{pqrs} = \langle\Psi|\hat{a}_p^\dagger\hat{a}_q^\dagger\hat{a}_s\hat{a}_r|\Psi\rangle \tag{5}$$

$$= \sum_{ij} C_i C_j \langle D_i|\hat{a}_p^\dagger\hat{a}_q^\dagger\hat{a}_s\hat{a}_r|D_j\rangle \tag{6}$$

from which the one-body reduced density matrix can be found as

$$\gamma_{pq} = \langle\Psi|\hat{a}_p^\dagger\hat{a}_q|\Psi\rangle \tag{7}$$

$$= \frac{1}{N-1}\sum_a \Gamma_{paqa} \tag{8}$$

An unbiased sampling of these quantities demands the introduction of a second Walker ensemble, to which the population dynamics are applied separately, and the statistics acquired independently, from the first. This "replica" sampling eliminates biasing by ensuring that all the required products of determinant amplitudes are calculated from populations from *both* simulations, and this sampling has found application in a variety of related Monte Carlo techniques.[50−52]

The reduced density matrices allow for the calculation of a host of molecular properties, including electrical moments, forces, and coupling to two-particle geminal functions;[48,49,53] however, their chief use in this present study is in their access to the gradient **g** and Hessian **H** of the energy, with respect to the orbital parameters:

$$g_{pq} = \frac{\partial E}{\partial \kappa_{pq}} = \langle\Psi|[\hat{E}_{pq}^-, \hat{\mathcal{H}}]|\Psi\rangle \tag{9}$$

and

$$H_{pq,rs} = \frac{\partial^2 E}{\partial \kappa_{pq}\partial \kappa_{rs}} \tag{10}$$

$$= \frac{1}{2}(1 + \hat{P}_{pq,rs})\langle\Psi|[\hat{E}_{pq}^-, [\hat{E}_{rs}^-, \hat{\mathcal{H}}]]|\Psi\rangle \tag{11}$$

in which the operator $\hat{P}_{pq,rs}$ permutes the orbital pair indices pq and rs, and $\hat{\mathcal{H}}$ is the relevant Hamiltonian.[1,10,34,35] These objects may be expressed entirely in terms of the reduced density matrices and the one- and two-electron integrals, $\{h_{pq}\}$ and $\{\langle pq \| rs\rangle\}$, in much the same manner as the analogous quantities are formulated in Hartree−Fock theory. Indeed, convergence is defined when the gradient vanishes, at which point the generalized Brillouin theorem is satisfied, indicating that there is no interaction between the CASSCF wave function and its singly excited configurations.

The energies presented in this work are quasi-variational energy estimates, derived from these sampled density matrices, and given by

$$E = \sum_{pq} h_{pq}\gamma_{pq} + \sum_{p>q,r>s} \Gamma_{pqrs}\langle pq\|rs\rangle + h_{nuc} \tag{12}$$

This ensures that consistency with the corresponding gradient and Hessian expressions is maintained. However, it would be instructive in a future study also to consider two other, nonvariational energy expressions commonly used in FCIQMC, derived from a mixed estimator and the "shift", which is a measure of the offset required to yield a norm-conserving propagator.[20]

Although the matrix $\boldsymbol{\kappa}$ may be obtained by solution of the stationary equation

$$\mathbf{H}\boldsymbol{\kappa} = -\mathbf{g} \qquad (13)$$

convergence is improved by instead constructing the *augmented* Hessian and its corresponding eigenequation.[54,55] Thus, $\boldsymbol{\kappa}$ is found as the lowest root of the equation

$$\begin{pmatrix} 0 & \mathbf{g}^T \\ \mathbf{g} & \mathbf{H}/\lambda \end{pmatrix}\begin{pmatrix} 1/\lambda \\ \boldsymbol{\kappa} \end{pmatrix} = \epsilon\begin{pmatrix} 1/\lambda \\ \boldsymbol{\kappa} \end{pmatrix} \qquad (14)$$

with $\epsilon = \lambda \mathbf{g}^\dagger \boldsymbol{\kappa}$, whose solution is found at modest computational expense via iterative subspace methods, as implemented in the PySCF package.[56]

The protocol outlined above represents a single macroiterative cycle—a single FCIQMC convergence and update of the CASSCF energy and orbital coefficients. Once performed, the newly obtained orbitals and transformed integrals are used to construct a new Hamiltonian, and the process continued until the desired convergence is achieved. The initial studies to which we now turn to address the suitability of this approach for achieving meaningful and satisfactory convergences of this type, and exactly what level of convergence can be expected of the macroiterations in the presence of random errors in the sampled energy, gradient, and Hessian expressions.

RESULTS AND DISCUSSION

Preliminary Studies. The natural first test for this new formulation is the comparison with entirely deterministic calculations. In principle, this should provide the same results as an approach using conventional CI theory for the configurational optimizer, and a comparison between the two thus yields some insight into the effects of the inevitable introduction of stochastic noise up to the convergence. As concrete examples, we turn to the benzene and naphthalene molecules in their experimental equilibrium geometries and in cc-pVDZ basis sets.[57,58] The active spaces in these cases are (6,6) and (10,10), respectively, for which the diagonalization of the active Hamiltonian is straightforward.

Of particular concern for the stochastic formulation is the satisfactory sampling of the density matrices. We return to a consideration of the behavior with number of walkers (N_w) for the later systems, but our initial focus with these smaller molecules is to assess the effect of the number of iterations of the FCIQMC dynamic for the accurate accumulation of the density matrices for these purposes, and the effect of this sampling time on the overall convergence.

The convergence of the CASSCF macroiterations as the number of FCIQMC iterations, N_{RDM}, for which the density matrices are sampled changes is shown in Figure 1. These RDMs are sampled fresh every macroiteration, and no prior initialization information is currently used between macroiteration steps, although the potential benefits of so doing are to be investigated in future studies. It can be seen that the overall qualitative convergence profile of the macroiterations are relatively insensitive to the length of time sampling the density matrices. At each FCIQMC iteration, each walker has the possibility to sample only a single contribution to the sum in eq 6 if a doubly excited walker is *successfully* spawned, and will contribute N terms if a singly excited walker is created. It further contributes N^2 (diagonal) terms during the course of a configuration being occupied (this is accumulated and only included once during the lifetime of the determinant for
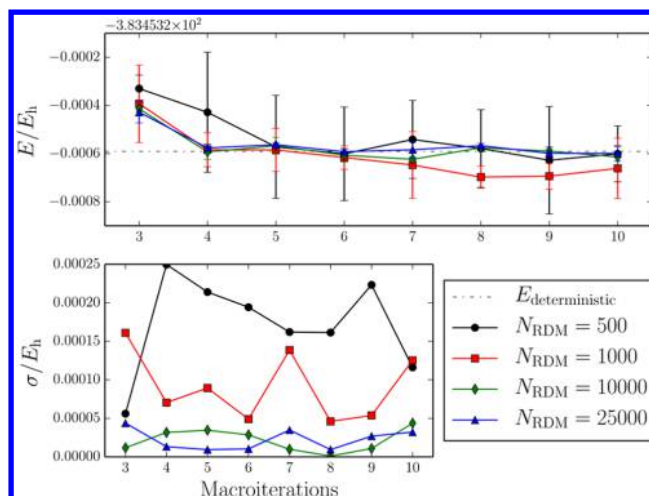

Figure 1. Final stages of the macroiterative convergence for a (10,10) naphthalene calculation in a cc-pVDZ basis, with the configurational optimizations performed over different numbers of density-matrix sampling iterations and using 10^4 walkers. The error bars are obtained as the standard deviation (σ) of three independent simulations (not standard error), initialized with different random number seeds, and these are plotted in the lower panel. Too few iterations make for noisy results, but the calculations performed with 25 000 sampling events are much more consistent and converge to the deterministic result with satisfactorily small deviations, once converged.

computational expediency; see ref 48 for more details). The fact that as few as 500 sampling iterations with 10^4 walkers (and a successful spawning rate of ∼1%) can provide qualitatively correct results, therefore, demonstrates an efficient sampling for these purposes. This is substantially helped by the fact that the diagonal (generally dominant) part of the two-body RDM is averaged over the stochastic wave function *exactly* for the sampling iterations, without requiring an additional stochastic step, as is required for the off-diagonal elements in eq 6. Furthermore, any deterministic space defined as part of the "semistochastic" adaptation of the algorithm (which generally contains some of the largest weighted configurations) has its contribution to the density matrices included exactly.[46−48] Whether this robust sampling is maintained or more iterations are required for systems with larger degrees of static correlation remains an open question, although this is likely offset by the larger number of walkers also required to resolve the wave function.

Despite the similarity and robustness of the qualitative results, the number of sampling iterations does have the expected effect on the standard deviation in the energy estimator over independent samples at each macroiteration. The variation between independent calculations, as measured by the standard deviations in Figure 1, can be traced to two effects due to the stochastic error in the density matrices. The first is the random error in the calculation of the variational energy for a given macroiteration, as given by eq 12, while the second is in the random error in the gradient and Hessian information in previous iterations, which gives different updates for the $\boldsymbol{\kappa}$ matrix and, therefore, orbital spaces in each macroiteration. Both of these effects are systematically controllable by changing both N_{RDM} and N_w. Too few sampling iterations of the density matrices (N_{RDM}) yields noisy behavior, and a standard deviation between independent calculations of up to 0.5 mE$_h$. Increasing the sampling decreases the changes

between energies at each macroiteration as expected. The ultimate convergence criterion for the optimization of the overall wave function must be greater than this standard deviation, since, even at "convergence", it is expected that the parameters will vary in a random fashion on the order of this standard deviation. For this reason, the choice of 25 000 sampling iterations is chosen for the rest of the results in this work, to provide close agreement with the fully deterministic result, and allows for a convergence threshold on the order of ± 0.1 mE$_h$.

Having established that the density matrices can be obtained with sufficient quality for the orbital optimization step, we may compare the specific behavior of the stochastic convergence with that of its deterministic counterpart, as given in Figure 2.
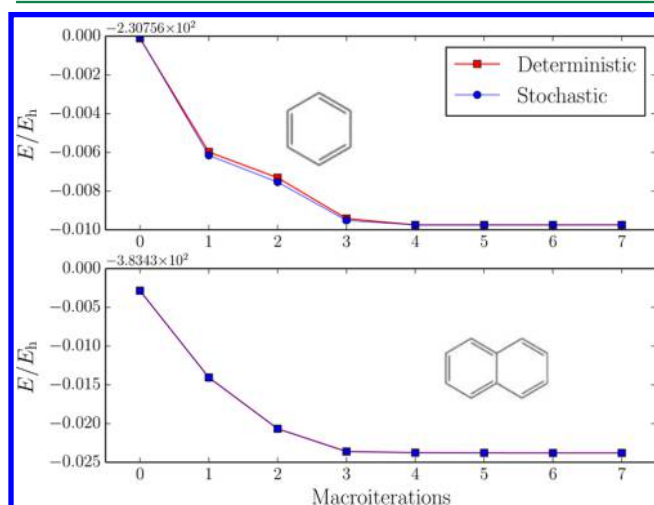

Figure 2. Convergence of (6,6) and (10,10) calculations for benzene (upper panel) and naphthalene (lower panel) respectively, illustrating the close agreement between the deterministic and stochastic formulations. The energy of each stochastic macroiteration is given as the average of those of three independent calculations, and the error bars by the corresponding standard deviations. In both the (6,6) and the (10,10) examples, the convergence was achieved with $O[10^5]$ walkers for each FCIQMC calculation. The zeroth iteration corresponds to the CASCI energy where the active orbital space is composed of canonical Hartree−Fock orbitals, demonstrating the additional effect of the orbital optimization for these systems.

The conclusion borne out by these results appears to be that, once the density matrices are resolved with sufficient clarity, the stochastic noise inherent in this new formulation does not particularly change the convergence of the energy over that of the conventional approach. The stochastic method clearly does demand a somewhat more permissive convergence criterion than its deterministic cousin—on the order of 10^{-4}−10^{-5} E$_h$, as established above—but the sub-millihartree agreement with deterministic results (where comparison is possible) suggests the feasibility of this new approach for addressing questions of physical and chemical significance.

As an initial illustration of such problems, we consider the torsional barrier of the ethene molecule, C_2H_4, as an archetypal example of the type of substantial static correlation problem to which CASSCF is traditionally best-suited.[59] In this case, the bonding and antibonding π and π^* orbitals become degenerate as the dihedral angle (ϕ) approaches 90°, and a proper treatment of the twisted geometry thus demands contributions

from both the π^2 and the π^{*2} configurations to give rise to a diradical singlet.

Figure 3 details the description of the torsional barrier by various levels of theory, and it illustrates an important
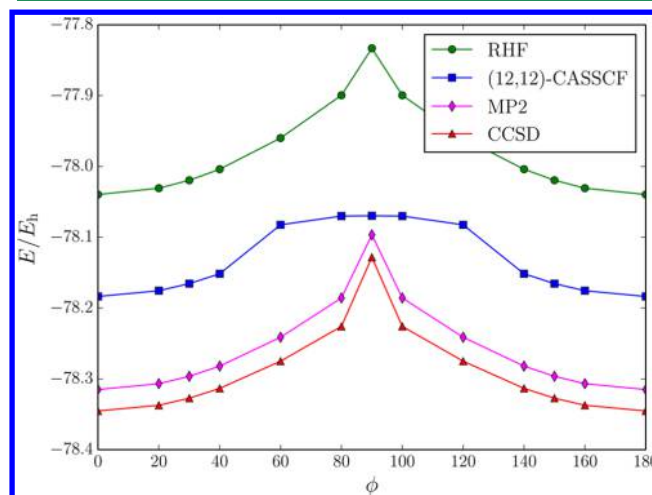

Figure 3. Torsional barrier of the ethene molecule in a cc-pVDZ basis set at various levels of theory, with all other geometrical parameters held at their equilibrium experimental values.[57] Cusp behavior indicates the inability to address the strong correlation effects that give rise to a diradical singlet character of the molecule at dihedral angles of 90°. The FCIQMC-CASSCF approach can consistently optimize the orbitals along this reaction coordinate in the presence of strong correlation effects, with $O[10^6]$ walkers.

advantage of the CASSCF approach in its ability to eliminate the energetic cusp at $\phi = 90°$. This cusp appears in the restricted HF curve as a result of that theory's complete neglect of the excited configuration, and the inconsistent treatment of this state by both CCSD and MP2 fails to remove this feature completely. By contrast, the CASSCF allows for the necessarily equal contributions from the π^2 and the π^{*2} configurations at the barrier and, hence, achieves the smooth curve required for a qualitatively correct description of the behavior. This also demonstrates the ability for the FCIQMC-CASSCF to also work in situations with changing levels of correlation, robustly and consistently optimizing the orbitals across the potential energy curve.

Toward Extended Systems. The ethene molecule provides a useful, albeit simple, illustration of the general importance of treating the full π-valence space when considering π-electron systems. However, the formulation introduced here is applicable to active spaces of much greater size, and it is to these more extended systems that our attention now turns.

The polycyclic aromatic hydrocarbons, formed of fused six-membered rings,[26,27] have long been a focus of both experimental and theoretical interest,[28,60−69] providing technological potential,[24,25,70] as well as being a source of medical and environmental concern.[71−73] The linear acenes have been extensively studied with DMRG,[28,29] as their quasi-one-dimensional structure is ideally suited to the method. However, an advantage of FCIQMC is that its efficiency is not particularly dependent on the dimensionality of the system. As exemplar problems of this new technique, therefore, we explore a series of nonlinear polycyclic aromatic hydrocarbons in cc-pVDZ basis sets,[58] up to the coronene—or superbenzene—molecule,

taking in the full carbon π-system in each case. This allows for a balanced active space for comparison between the systems as they increase in size, without truncation of the conjugated electrons. The geometries used are optimized at the density functional theory level,[74−76] using the B3LYP functional.[77−80]

Following from the benzene and naphthalene studies of the previous section, we first consider the phenanthrene and triphenylene molecules, with (14,14) and (18,18) active spaces, respectively. This latter system is beyond the reach of deterministic CASSCF theories but, as illustrated in Figure 4, the stochastic formulation provides a smooth, robust convergence.
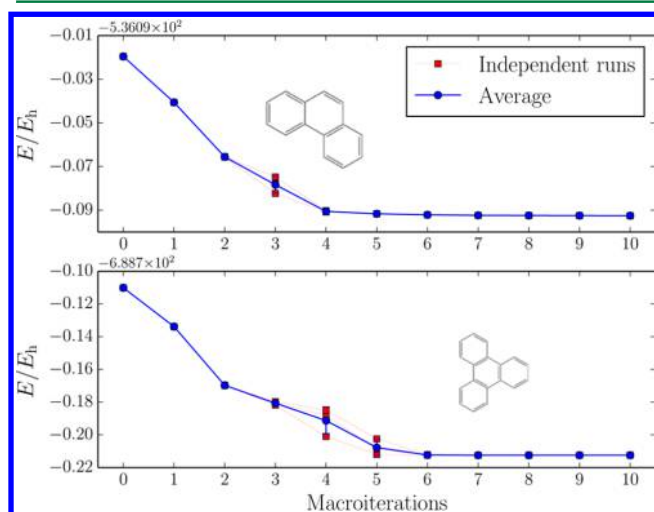

Figure 4. Macroiterative convergences for phenanthrene (upper panel) and triphenylene (lower panel) in a cc-pVDZ basis.[58] The phenanthrene system is studied with a (14,14) active space, in a total space of 246 orbitals, whereas, for triphenylene, we adopt an (18,18) active space in the 312-orbital total space. Each configuration iteration was allowed to evolve after equilibration for 25 000 density-matrix sampling iterations. The curves shown in red detail the results of independent calculations, initialized with different random number seeds, while those shown in blue plot the averages of these simulations. While the independent convergences follow rather different trajectories, their latter iterations are in sufficient agreement with each other to give a small error bar for the obtained energy.

The energy for each macroiteration is obtained directly from the reduced density matrices, as depicted in eq 12; as in the previous section, we calculate an average energy for each point from the results of three independent calculations, initialized from different random number seeds, with the corresponding standard deviation serving as the error bar. As can be seen from Figure 4, the precise trajectories of the independent convergences differ somewhat in their initial phases, as small random errors in the gradients and Hessians lead to propagation of differing orbitals through the macroiterative optimization. However, the later iterations agree sufficiently well, such that a meaningful energy and error bar may be extracted, providing confidence that the same orbital space is sampled at convergence. In particular, it is evident that performing each configurational step for 25 000 density-matrix sampling iterations after an equilibration period—the rule of thumb inferred in the previous section—is sufficient for the robust, reliable convergence, which is our objective. In addition, walker populations were chosen such that the population residing on the reference exceeded 5×10^4, which has

previously been shown to be a satisfactory criterion for reliable convergence of any initiator error for systems with substantial weight on a single determinant.[41,43,45] This results in small changes to the total number of walkers for each iteration, as the wave function sparsity alters as the orbitals change. However, this was found to give consistently converged results for these systems, and we now turn to a more detailed consideration of the number of walkers required for larger active spaces in the coronene molecule.

The Effect of the Number of Walkers. It has been stressed that the macroiterative optimization of the orbitals in CASSCF is a nonlinear problem; as such, ensuring convergence to a global minimum is almost impossible, while sensitivity to initial conditions or simulation procedure can lead to different solutions. One way in which convergence to global minima is encouraged in nonlinear optimization problems is somewhat counterintuitively, via the addition of random noise into the gradient and Hessian in an optimization step. An example of this is the essential addition of "noise" to the optimization in DMRG, where a nonlinear factorization of the wave function coefficients is optimized.[33,81] Although the added noise in DMRG is not generally stochastic (although it can be), neglect of this noise can lead to the convergence to metastable solutions and local minima, rather than the desired converged state.[81] With this in mind, we detail the three anticipated effects of increasing the number of walkers in the FCIQMC-CASSCF procedure.

First among these will be the decrease in "initiator error" in the FCIQMC calculation.[38] The use of the initiator approximation (applied throughout this work) entails the introduction of a systematically improvable error into the sampling of the wave function as a way of encouraging annihilation events and ameliorating the sign problem in the space. As the number of walkers increases, it can be rigorously shown that the energy (generally rapidly) converges to the exact (FCI) result. Second, the increase in the number of walkers will lead to a reduction in the error in the sampled density matrices (and, hence, the gradient and Hessian of the orbital rotations), again tending to an exact limit. This is due both to a reduction in the initiator error in the wave function from which the density matrices are sampled, and also an improvement in the sampling of the matrices themselves. However, a third effect of changing the number of walkers is related to the convergence profile in the nonlinear optimization of the orbitals. As the number of walkers increases, it will decrease the random noise in the sampled gradient and Hessian information for the orbital rotation steps; this will influence the stability of the global optimization of the orbitals.

The convergences for coronene, using a (24,24) active space and different values for N_w, are shown in Figure 5. The number of active space determinants is $O[10^{12}]$. The simulations that are carried out with 100 and 200 million walkers per FCIQMC calculation (the latter value of which fulfils the criterion of placing 5×10^4 walkers upon the reference) provide the type of smooth, robust convergences in close agreement with each other that we observe for the smaller systems. Although slightly different optimization pathways may be taken, these walker numbers both achieve a quantitative agreement at convergence within a small standard deviation of each other. However, a calculation using only 10 million walkers for each step results in a very different convergence to a lower-energy solution, in marked disagreement with the other results.
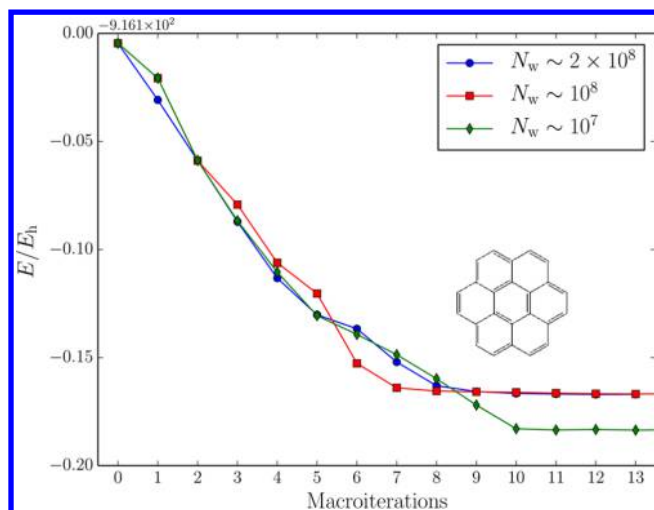
Figure 5. Convergences for the coronene molecule in a cc-pVDZ basis, using different walker populations, N_w, for each configurational optimization, in a (24,24) active space chosen from a 396-orbital total space. Walker populations over 50 million result in robust convergence to a metastable state, but an undersampled calculation using $N_w \approx 10^7$ yields a lower-energy orbital solution. This solution can then be refined by increasing the number of walkers (see Figure 7).

This discrepancy is not merely a simple manifestation of initiator error, but rather a clear example of the sensitivity of the optimization to its initial and early conditions. As Figure 6
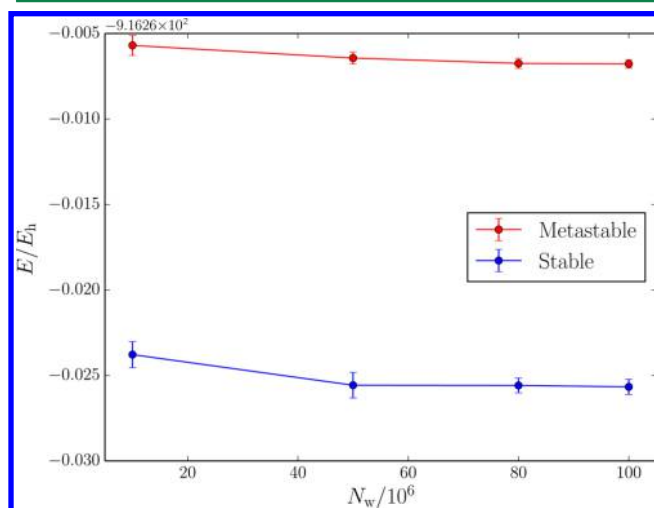

Figure 6. FCIQMC energies for the metastable (red) and stable (blue) states found for coronene, using the converged orbitals from separate CASSCF optimizations with different walker populations (N_w). The metastable orbitals correspond to the optimization at 200 million walkers, while the stable state corresponds to 10 million walkers, as shown in Figure 5. The removal of initiator error, as N_w is increased, decreases the energy of both states, but is not sufficient to explain the discrepancy between the two.

illustrates, increasing the number of walkers in FCIQMC calculations to eliminate any effects of initiator error using the converged orbitals of both the metastable (higher energy) and stable (lower energy) states decreases their energy as the initiator error is removed, but the two states remain well-separated by ~20 mE$_h$, while the initiator error is <2 mE$_h$.

Therefore, it appears that rather noisy initial macroiterations may, in fact, be advantageous in converging upon a true ground

state, much in the manner that added noise is helpful for DMRG. Indeed, in Figure 7, we adopt a protocol wherein the
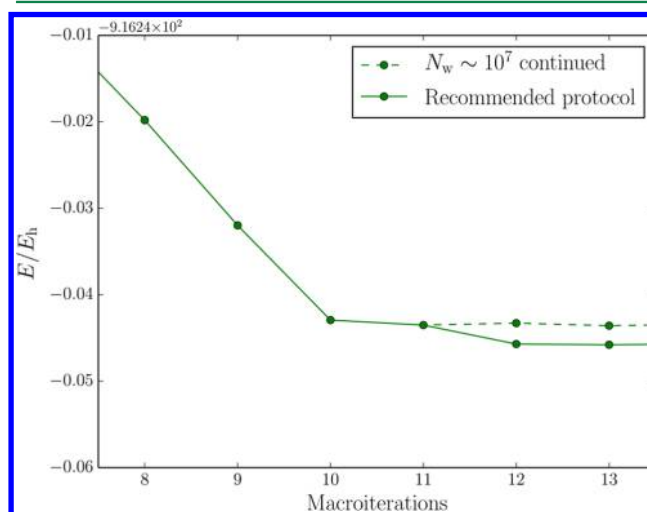

Figure 7. Convergence for the (24,24) coronene system with the initial macroiterations performed using 10^7 walkers, and those after and including macroiteration 12 using 10^8, yielding a result in agreement with the analysis of Figure 6. The dashed curve illustrates the trajectory if a walker population of $O[10^7]$ is maintained in these latter stages, giving an indication of the initiator error encountered upon so doing.

first configurational optimizations are performed with $O[10^7]$ walkers, and macroiteration 12 and later steps with 100 million walkers to converge residual initiator error. This approach yields a trajectory toward the converged energy of the stable state in Figure 6, and is the recommended procedure for future studies to encourage convergence to the global minima of the orbital optimization problem. We speculate further that a deterministic FCI solver of the (24,24) coronene problem (if possible) with the same CASSCF algorithm would also likely converge to the higher-energy orbital solution, and that for large active spaces or in the presence of strong correlation and difficult convergence, the addition of artificial noise to the CASSCF optimization may also yield benefits in convergence stability. The protocol of optimizing first at lower walker numbers also reduces the computational cost of an FCIQMC-CASSCF calculation, since only a few final iterations are required at the higher walker number finally to eliminate initiator error. While the optimization is weakly exponentially scaling with the number of orbitals and electrons in the active space,[40,41,44,82] in the example of the (24,24) coronene system in Figure 7, this corresponded to only 12 h on 320 cores per macroiteration (including savings due to symmetry), taking advantage of the highly parallelizable nature of the FCIQMC algorithm. Memory requirements were also small, at ~3 GB of distributed memory (in contrast to the unfeasible traditional calculation, which would require a minimum of ~100TB of RAM).

The Electronic Structure of Polycyclic Hydrocarbons from FCIQMC-CASSCF. Further insight into the electronic structure of these systems may be gleaned by considering the natural orbital occupation numbers, $\{n_i\}$, of the converged wave functions. Integrated measures of the number of "effectively unpaired" electrons in a system have been proposed by Takatsuka,[83−87] as

$$N_{\text{unpaired}}^{(T)} = \sum_i (2n_i - n_i^2) \qquad (15)$$

and by Head-Gordon,[88−90] as

$$N_{\text{unpaired}}^{(HG)} = \sum_i \min(n_i, 2 - n_i) \qquad (16)$$

in which $0 \leq n_i \leq 2$. In addition, the HONO−LUNO gap, $n_{\text{HONO}} - n_{\text{LUNO}}$, can be used, where HONO and LUNO correspond to the highest/lowest occupied/unoccupied natural orbital, respectively. This quantity should not be considered as a measure of an energetic excitation, but rather as a metric for the deviation from the suitability of a Hartree−Fock picture of the electronic wave function. As noted previously,[28,29] a little care must also be exercised in interpreting the values of N_{unpaired}; certainly, they should not be taken literally as the number of unpaired electrons found in a given system, but, taken together with $n_{\text{HONO}} - n_{\text{LUNO}}$, provide a useful indication of the correlated effects present in differently sized molecules.

Figure 8 compares these metrics for the 2D systems discussed thus far to the corresponding linear acenes, which
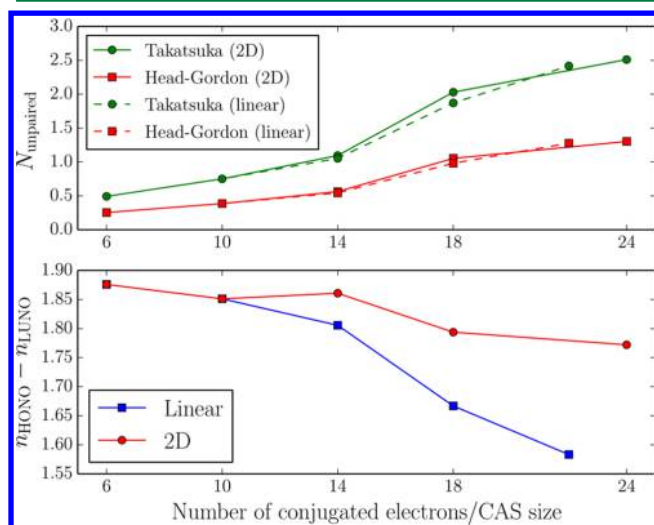

Figure 8. Integrated metrics $N_{\text{unpaired}}^{(HG)}$ and $N_{\text{unpaired}}^{(T)}$, along with the HONO−LUNO gaps, for the two-dimensional (2D) systems considered here, compared with the series of linear acenes of similar size.

we have also calculated. The trend for the linear systems reveals, as has been previously reported,[28] the steady increase in correlated behavior as the chain length (and CAS size) is increased, leading to increasingly polyradical character of the wave function. However, the behavior for the 2D systems is rather less straightforward, indicating that the strength of the correlation effects and radical nature of the resulting wave function is not simply related to the number of π electrons in the conjugated system, but also to the precise geometry of the molecule under study. While the integrated measure of the radical character is approximately the same for the 1D and 2D structures when comparing the same number of conjugated electrons, the HONO−LUNO gap does not increase at the same rate.

This behavior can be rationalized by examining the occupation number spectra, as shown in Figure 9 for linear tetracene and 2D triphenylene, which have the same number of electrons in its π-system. These exemplar spectra highlight that,
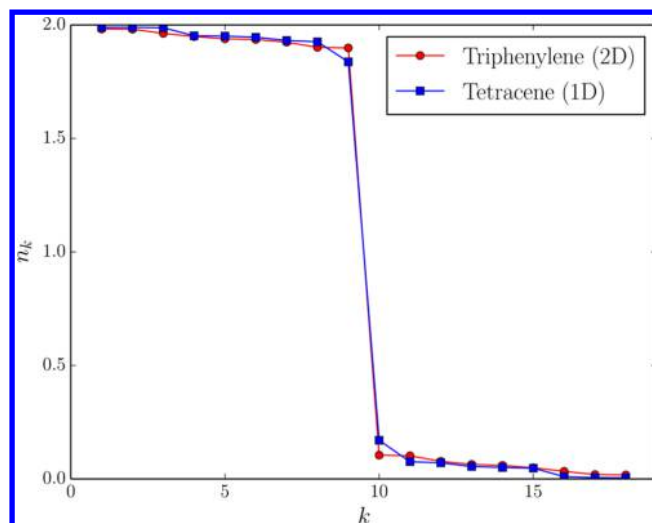

Figure 9. Natural orbital occupation numbers for the (18,18) active spaces of tetracene and triphenylene, illustrating the degeneracy of the HONO and LUNO in the 2D case, which is not present in the linear system.

while the HONO-LUNO gap of the linear system is smaller than that of the 2D case, the latter system sees the emergence of degeneracy in both the HONO and the LUNO not present in the former, contributing to the integrated measures of the radical nature. This is expected due to the increased symmetry of the 2D system, as compared to the linear acene. It has previously been shown that the radical HONO and LUNO orbitals are related to *edge* effects of these conjugated systems, with larger systems exhibiting HONO and LUNO orbitals in these systems, which increasingly localize onto the perimeter of conjugated system.[29] This rationalizes the results of Figure 8, where the smaller perimeter of the 2D systems, compared to the linear acenes for the same number of π electrons, is reflected in the size of the HONO−LUNO gap. Visualization of the coronene HONO in Figure 10 also indicates that these orbitals that are most radical in nature are indeed beginning to localize on the edge of the molecule. It is anticipated that the increased degeneracy of the 2D conjugated systems will mean that, for a given *perimeter* of these systems, the 2D systems will
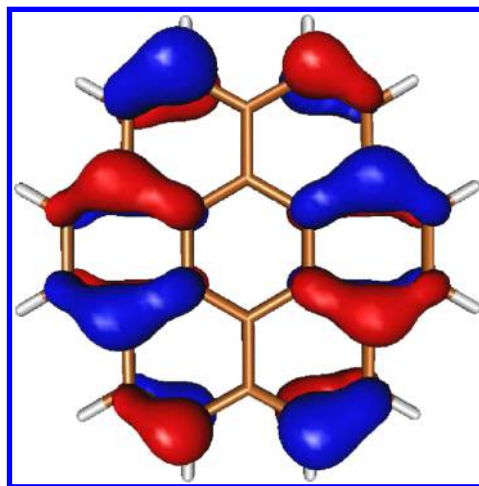

Figure 10. Visualization of the highest-occupied natural orbital (HONO) for coronene,[91] illustrating the accumulation of electron density around the outer carbon sites.

exhibit stronger correlation effects than their one-dimensional (1D) counterparts. Theoretically observing these correlated trends provides a stern challenge for future applications of this new approach. However, the applicability and relative ease in dealing with these large correlated spaces with a stochastic solver bodes well for its future utility and scope to probe these systems.

CONCLUSIONS

A novel formulation of multiconfigurational self-consistent field theory, using a two-step, macroiterative algorithm with full configuration interaction quantum Monte Carlo (FCIQMC) methodology for its configurational optimizations, is capable of performing successful calculations with large active spaces. In this work, this ability is demonstrated with a study of a series of two-dimensional (2D) polycyclic aromatic hydrocarbons, culminating in calculations on the coronene molecule with a (24,24) active space.

The inevitable introduction of stochastic noise in this approach does not significantly worsen convergence over a deterministic method, provided that satisfactory sampling is undertaken. In particular, we observe that the FCIQMC calculations must be performed for sufficiently many density-matrix sampling iterations (with 25 000 being a useful, if informal, lower bound) and with sufficiently many walkers if the adverse effects of errors in the density matrices are to be avoided. Moreover, it is shown that the noise created by using comparatively few walkers for the initial iterations can be of benefit in converging to a true ground state, with high populations only required in the last stages of convergence in order to provide a satisfactory treatment of initiator error. The modest computational resources thus required suggest that larger active spaces will still be within range, and thus that major new avenues of inquiry—including studies of transition-metal compounds and clusters—are now open and navigable. Furthermore, an approach for obtaining excited states within FCIQMC will allow for a *state-averaged* CASSCF implementation in the future, allowing for studies of excitations and photochemistry in correlated molecules.[92]

AUTHOR INFORMATION

Corresponding Authors
*E-mail: ret41@cam.ac.uk (R. E. Thomas).
*E-mail: george.booth@kcl.ac.uk (G. H. Booth).
Notes
The authors declare no competing financial interest.

ACKNOWLEDGMENTS

REFERENCES

(1) Helgaker, T.; Jørgensen, P.; Olsen, J. *Molecular Electronic-Structure Theory*; John Wiley & Sons: Chichester, U.K., 2000.
(2) Roos, B. O. *Chem. Phys. Lett.* **1972**, *15*, 153.
(3) Hinze, J. *J. Chem. Phys.* **1973**, *59*, 6424.
(4) Siegbahn, P. E. M.; Heiberg, A.; Roos, B. O.; Levy, B. *Phys. Scr.* **1980**, *21*, 323.

(5) Roos, B. O.; Taylor, P. R.; Siegbahn, P. E. M. *Chem. Phys.* **1980**, *48*, 157.
(6) Siegbahn, P. E. M.; Almlöf, J.; Heiberg, A.; Roos, B. O. *J. Chem. Phys.* **1981**, *74*, 2384.
(7) Knowles, P. J.; Werner, H.-J. *Chem. Phys. Lett.* **1985**, *115*, 259.
(8) Werner, H.-J.; Knowles, P. J. *J. Chem. Phys.* **1985**, *82*, 5053.
(9) Olsen, J. *Int. J. Quantum Chem.* **2011**, *111*, 3267.
(10) Lin, C.; Demkov, A. A. *Phys. Rev. B: Condens. Matter Mater. Phys.* **2014**, *90*, 235122.
(11) Andersson, K.; Malmqvist, P.-Å; Roos, B. O. *J. Chem. Phys.* **1992**, *96*, 1218.
(12) Werner, H.-J.; Knowles, P. J. *J. Chem. Phys.* **1988**, *89*, 5803.
(13) Shamasundar, K. R.; Knizia, G.; Werner, H.-J. *J. Chem. Phys.* **2011**, *135*, 054101.
(14) Olsen, J.; Roos, B. O.; Jørgensen, P.; Jensen, H. J. Aa. *J. Chem. Phys.* **1988**, *89*, 2185.
(15) Malmqvist, P.-Å; Rendell, A.; Roos, B. O. *J. Phys. Chem.* **1990**, *94*, 5477.
(16) Fleig, T.; Olsen, J.; Marian, C. M. *J. Chem. Phys.* **2001**, *114*, 4775.
(17) Fleig, T.; Olsen, J.; Visscher, L. *J. Chem. Phys.* **2003**, *119*, 2963.
(18) Ma, D.; Li Manni, G.; Gagliardi, L. *J. Chem. Phys.* **2011**, *135*, 044128.
(19) Vogiatzis, K. D.; Li Manni, G.; Stoneburner, S. J.; Ma, D.; Gagliardi, L. *J. Chem. Theory Comput.* **2015**, *11*, 3010.
(20) Booth, G. H.; Thom, A. J. W.; Alavi, A. *J. Chem. Phys.* **2009**, *131*, 054106.
(21) Neuhauser, D.; Rabani, E.; Baer, R. *J. Chem. Theory Comput.* **2013**, *9*, 24.
(22) Willow, S. Y.; Kim, K. S.; Hirata, S. *J. Chem. Phys.* **2013**, *138*, 164111.
(23) Neuhauser, D.; Gao, Y.; Arntsen, C.; Karshenas, C.; Rabani, E.; Baer, R. *Phys. Rev. Lett.* **2014**, *113*, 076402.
(24) Smith, M. B.; Michl, J. *Annu. Rev. Phys. Chem.* **2013**, *64*, 361–386.
(25) Teichen, P. E.; Eaves, J. D. *J. Phys. Chem. B* **2012**, *116*, 11473–11481.
(26) Clar, E. *Polycyclic Hydrocarbons*; Academic Press: London, 1964.
(27) Havey, R. G. *Polycyclic Aromatic Hydrocarbons*; Wiley–VCH: New York, 1997.
(28) Hachmann, J.; Dorando, J. J.; Avilés, M.; Chan, G. K.-L. *J. Chem. Phys.* **2007**, *127*, 134309.
(29) Mizukami, W.; Kurashige, Y.; Yanai, T. *J. Chem. Theory Comput.* **2013**, *9*, 401.
(30) Werner, H.-J. *Adv. Chem. Phys.* **1987**, *69*, 1.
(31) Shepard, R. *Adv. Chem. Phys.* **1987**, *69*, 63.
(32) Schmidt, M. W.; Gordon, M. S. *Annu. Rev. Phys. Chem.* **1998**, *49*, 233.
(33) Zgid, D.; Nooijen, M. *J. Chem. Phys.* **2008**, *128*, 144116.
(34) Ghosh, D.; Hachmann, J.; Yanai, T.; Chan, G. K.-L. *J. Chem. Phys.* **2008**, *128*, 144117.
(35) Yanai, T.; Kurashige, Y.; Ghosh, D.; Chan, G. K.-L. *Int. J. Quantum Chem.* **2009**, *109*, 2178.
(36) Yanai, T.; Kurashige, Y.; Neuscamman, E.; Chan, G. K.-L. *J. Chem. Phys.* **2010**, *132*, 024105.
(37) Kurashige, Y.; Chan, G. K.-L.; Yanai, T. *Nat. Chem.* **2013**, *5*, 660.
(38) Cleland, D. M.; Booth, G. H.; Alavi, A. *J. Chem. Phys.* **2010**, *132*, 041103.
(39) Booth, G. H.; Alavi, A. *J. Chem. Phys.* **2010**, *132*, 174104.
(40) Booth, G. H.; Cleland, D. M.; Thom, A. J. W.; Alavi, A. *J. Chem. Phys.* **2011**, *135*, 084104.
(41) Cleland, D. M.; Booth, G. H.; Overy, C.; Alavi, A. *J. Chem. Theory Comput.* **2012**, *8*, 4138.
(42) Booth, G. H.; Grüneis, A.; Kresse, G.; Alavi, A. *Nature* **2012**, *493*, 365.
(43) Thomas, R. E.; Overy, C.; Booth, G. H.; Alavi, A. *J. Chem. Theory Comput.* **2014**, *10*, 1915.
(44) Booth, G. H.; Smart, S. D.; Alavi, A. *Mol. Phys.* **2014**, *112*, 1855.

(45) Thomas, R. E.; Booth, G. H.; Alavi, A. *Phys. Rev. Lett.* **2015**, *114*, 033001.

(46) Petruzielo, F. R.; Holmes, A. A.; Changlani, H. J.; Nightingale, M. P.; Umrigar, C. J. *Phys. Rev. Lett.* **2012**, *109*, 230201.

(47) Blunt, N. S.; Smart, S. D.; Kersten, J. A.-F.; Spencer, J. S.; Booth, G. H.; Alavi, A. *J. Chem. Phys.* **2015**, *142*, 184107.

(48) Overy, C.; Booth, G. H.; Blunt, N. S.; Shepherd, J. J.; Cleland, D. M.; Alavi, A. *J. Chem. Phys.* **2014**, *141*, 244117.

(49) Thomas, R. E.; Opalka, D.; Overy, C.; Knowles, P. J.; Alavi, A.; Booth, G. H. *J. Chem. Phys.* **2015**, *143*, 054108.

(50) Zhang, S.; Kalos, M. H. *J. Stat. Phys.* **1993**, *70*, 515.

(51) Blunt, N. S.; Rogers, T. W.; Spencer, J. S.; Foulkes, W. M. C. *Phys. Rev. B: Condens. Matter Mater. Phys.* **2014**, *89*, 245124.

(52) Blunt, N. S.; Alavi, A.; Booth, G. H. *Phys. Rev. Lett.* **2015**, *115*, 050603.

(53) Booth, G. H.; Cleland, D. M.; Alavi, A.; Tew, D. P. *J. Chem. Phys.* **2012**, *137*, 164112.

(54) Lengsfield, B. H., III. *J. Chem. Phys.* **1980**, *73*, 382.

(55) Lengsfield, B. H., III. *J. Chem. Phys.* **1982**, *77*, 4073.

(56) *PySCF, A Python Module for Quantum Chemistry.* See: https://github.com/sunqm/pyscf.git.

(57) Herzberg, G. *Molecular Spectra and Molecular Structure: III. Electronic Spectra and Electronic Structure of Polyatomic Molecules*; Van Nostrand: New York, 1966.

(58) Dunning, T. H., Jr. *J. Chem. Phys.* **1989**, *90*, 1007.

(59) Krylov, A. I.; Sherrill, C. D.; Byrd, E. F. C.; Head-Gordon, M. *J. Chem. Phys.* **1998**, *109*, 10669.

(60) Angliker, H.; Rommel, E.; Wirz, J. *Chem. Phys. Lett.* **1982**, *87*, 208.

(61) Kertesz, M.; Hoffmann, R. *Solid State Commun.* **1983**, *47*, 97.

(62) Kivelson, S.; Chapman, O. L. *Phys. Rev. B: Condens. Matter Mater. Phys.* **1983**, *28*, 7236.

(63) Wiberg, K. B. *J. Org. Chem.* **1997**, *62*, 5720.

(64) Houk, K. N.; Lee, P. S.; Nendel, M. *J. Org. Chem.* **2001**, *66*, 5517.

(65) Bendikov, M.; Duong, H. M.; Starkey, K.; Houk, K. N.; Carter, E. A.; Wudl, F. *J. Am. Chem. Soc.* **2004**, *126*, 7416.

(66) Bendikov, M.; Duong, H. M.; Starkey, K.; Houk, K. N.; Carter, E. A.; Wudl, F. *J. Am. Chem. Soc.* **2004**, *126*, 10493.

(67) Bendikov, M.; Wudl, F.; Perepichka, D. F. *Chem. Rev.* **2004**, *104*, 4891.

(68) Mondal, R.; Shah, B. K.; Neckers, D. C. *J. Am. Chem. Soc.* **2006**, *128*, 9612.

(69) Reddy, A. R.; Bendikov, M. *Chem. Commun.* **2006**, 1179−1181.

(70) Reese, C.; Roberts, M.; Ling, M.; Bao, Z. *Mater. Today* **2004**, *7*, 20.

(71) Samanta, S. K.; Singh, O. V.; Jain, R. K. *Trends Biotechnol.* **2002**, *20*, 243.

(72) Armstrong, B.; Hutchinson, E.; Unwin, J.; Fletcher, T. *Environ. Health Persp.* **2004**, *112*, 970.

(73) Srogi, K. *Environ. Chem. Lett.* **2007**, *5*, 169.

(74) Eckert, F.; Pulay, P.; Werner, H.-J. *J. Comput. Chem.* **1997**, *18*, 1473.

(75) Werner, H.-J.; Knowles, P. J.; Knizia, G.; Manby, F. R.; Schütz, M. *Wiley Interdiscip. Rev.: Comput. Mol. Sci.* **2012**, *2*, 242.

(76) *MOLPRO, Version 2012.1, a Package of Ab Initio Programs*; 2012. See: http://molpro.net.

(77) Vosko, S. H.; Wilk, L.; Nusair, M. *Can. J. Phys.* **1980**, *58*, 1200.

(78) Lee, C.; Yang, W.; Parr, R. G. *Phys. Rev. B: Condens. Matter Mater. Phys.* **1988**, *37*, 785.

(79) Becke, A. D. *J. Chem. Phys.* **1993**, *98*, 5648.

(80) Stephens, P. J.; Devlin, F. J.; Chabalowski, C. F.; Frisch, M. J. *J. Phys. Chem.* **1994**, *98*, 11623.

(81) White, S. R. *Phys. Rev. B: Condens. Matter Mater. Phys.* **2005**, *72*, 180403(R).

(82) Shepherd, J. J.; Scuseria, G. E.; Spencer, J. S. *Phys. Rev. B: Condens. Matter Mater. Phys.* **2014**, *90*, 155130.

(83) Takatsuka, K.; Fueno, T.; Yamaguchi, K. *Theor. Chim. Acta* **1978**, *48*, 175.

(84) Takatsuka, K.; Fueno, T. *J. Chem. Phys.* **1978**, *69*, 661.

(85) Bochicchio, R. C. *J. Mol. Struct.: THEOCHEM* **1998**, *429*, 229.

(86) Staroverov, V. N.; Davidson, E. R. *J. Am. Chem. Soc.* **2000**, *122*, 186.

(87) Staroverov, V. N.; Davidson, E. R. *Chem. Phys. Lett.* **2000**, *330*, 161.

(88) Head-Gordon, M. *Chem. Phys. Lett.* **2003**, *372*, 508.

(89) Head-Gordon, M. *Chem. Phys. Lett.* **2003**, *380*, 488.

(90) Bochicchio, R. C.; Torre, A.; Lain, L. *Chem. Phys. Lett.* **2003**, *380*, 486.

(91) Schaftenaar, G.; Noordik, J. H. *J. Comput.-Aided Mol. Des.* **2000**, *14*, 123.

(92) Blunt, N. S.; Smart, S. D.; Booth, G. H.; Alavi, A. *J. Chem. Phys.* **2015**, *143*, 134117.